Protein Science (1994), *3*:2073-2081. Cambridge University Press. Printed in the USA.

Docking of nitrogenase iron- and molybdenum-iron proteins for electron transfer and MgATP hydrolysis: The role of arginine 140 and lysine 143 of the *Azotobacter vinelandii* iron protein

LANCE C. SEEFELDT

Department of Chemistry and Biochemistry, Utah State University, Logan, Utah 84322-0300

(RECEIVED May 11, 1994; ACCEPTED June 29, 1994)

Abstract

Docking of the nitrogenase component proteins, the iron protein (FeP) and the molybdenum-iron protein (MoFeP), is required for MgATP hydrolysis, electron transfer between the component proteins, and substrate reductions catalyzed by nitrogenase. The present work examines the function of 3 charged amino acids, Arg 140, Glu 141, and Lys 143, of the *Azotobacter vinelandii* FeP in nitrogenase component protein docking. The function of these amino acids was probed by changing each to the neutral amino acid glutamine using site-directed mutagenesis. The altered FePs were expressed in *A. vinelandii* in place of the wild-type FeP. Changing Glu 141 to Gln (E141Q) had no adverse effects on the function of nitrogenase in whole cells, indicating that this charged residue is not essential to nitrogenase function. In contrast, changing Arg 140 or Lys 143 to Gln (R140Q and K143Q) resulted in a significant decrease in nitrogenase activity, suggesting that these charged amino acid residues play an important role in some function of the FeP. The function of each amino acid was deduced by analysis of the properties of the purified R140Q and K143Q FePs. Both altered proteins were found to support reduced substrate reduction rates when coupled to wild-type MoFeP. Detailed analysis revealed that changing these residues to Gln resulted in a dramatic reduction in the affinity of the altered FeP for binding to the MoFeP. This was deduced in FeP titration, NaCl inhibition, and MoFeP protection from Fe^{2+} chelation experiments. In addition, it was found that changing Arg 140 and Lys 143 to Gln resulted in a significant uncoupling of MgATP hydrolysis from intercomponent electron transfer rates between FeP and MoFeP. The wild-type complex was found to hydrolyze 2.5 MgATP per electron transferred, whereas the R140Q and K143Q proteins, when coupled to wild-type MoFeP, required 6 and 31 MgATP for each electron transferred, respectively. It is concluded that both Arg 140 and Lys 143 of the *A. vinelandii* nitrogenase FeP are important in the docking interaction with the MoFeP and that these residues probably function in aligning the FeP with the MoFeP for intercomponent electron transfer. A model is discussed in which these positively charged amino acids of the FeP might interact with negatively charged amino acids (Asp and Glu) on the MoFeP near its 8Fe cluster.

Keywords: electron transfer; iron protein; molybdenum-iron protein; MgATP hydrolysis; nitrogenase; protein docking; site-directed mutagenesis

Biological dinitrogen reduction is catalyzed by nitrogenase, a complex metalloenzyme consisting of the 2 separable component proteins, the molybdenum-iron protein and the iron protein (current reviews: Burris, 1991; Smith & Eady, 1992; Dean et al., 1993; Mortenson et al., 1993; Rees et al., 1993; Kim & Rees, 1994). The overall reaction of nitrogenase can be summarized, $1/2\text{MoFeP} + N_2 + 8H^+ + 8(\text{FeP}_r\text{-}2\text{MgATP}) \rightarrow 2NH_3 + H_2 + 1/2\text{MoFeP} + 8(\text{FeP}_{ox}\text{-}2\text{MgADP}) + 16P_i$, where FeP_r is the reduced state of FeP and FeP_{ox} is the 1-electron oxidized state of FeP. The MoFeP is the component responsible for substrate binding and reduction, which is thought to occur at its unique molybdenum-iron-sulfur-homocitrate containing cofactor (Kim & Rees, 1992b; Orme-Johnson, 1992). The MoFeP also contains 2 8Fe-(7-8)S clusters (Kim & Rees, 1992b; Bolin et al., 1993), which are thought to function as a reservoir of electrons for transfer to FeMoco during substrate reduction. The FeP, a ho-

Reprint requests to: Lance C. Seefeldt, Department of Chemistry and Biochemistry, Utah State University, Logan, Utah 84322-0300; e-mail: seefeldt@cc.usu.edu.

Abbreviations: FeP, nitrogenase iron protein; MoFeP, nitrogenase molybdenum-iron protein; FeP-MoFeP, iron protein-molybdenum-iron protein complex; FeMoco, iron-molybdenum cofactor; 8Fe cluster, 8Fe-(7-8)S or P cluster; TES, *N*-tris(hydroxymethyl)methyl-2-aminoethane sulfonic acid.

modimer, contains a single [4Fe-4S] cluster ligated between its subunits (Georgiadis et al., 1992). The FeP functions to transfer a low potential electron from its reduced $[4Fe\text{-}4S]^{1+}$ cluster to the MoFeP, probably the 8Fe cluster, with the concomitant hydrolysis of 2 MgATP to 2 MgADP (Mortenson et al., 1993). The mechanism of coupling MgATP hydrolysis to the electron transfer reaction remains unknown. The FeP is known to bind 2 MgATP per dimer with high affinity, but the hydrolysis of MgATP is only catalyzed by the complex of the FeP and the MoFeP. A minimum stoichiometry for the reaction is 2 MgATP molecules hydrolyzed for each electron transferred from the [4Fe-4S] cluster of the FeP to the MoFeP. The oxidized FeP, with 2 bound MgADP molecules, is released from the MoFeP in the reaction rate limiting step, and a new (FeP_r-2MgATP) complex binds to the MoFeP for a second electron transfer (Hageman & Burris, 1978; Thorneley & Lowe, 1985). This cycle is repeated until a sufficient number of electrons has been transferred for substrate reduction. The released (FeP_{ox}-2MgADP) complex is subsequently recycled by reduction (from flavodoxin or ferredoxin in vivo or dithionite in vitro) and the exchange of the 2 bound MgADP for 2 MgATP (Thorneley & Lowe, 1985).

Docking of the nitrogenase FeP and MoFeP is a prerequisite to all nitrogenase reactions including hydrolysis of MgATP, electron transfer, and substrate reduction. Little is presently known about this docking mechanism and the interactions that activate the enzyme for MgATP hydrolysis and electron transfer. Recent X-ray crystallographic analysis of both the MoFeP and the FeP from *Azotobacter vinelandii* (Georgiadis et al., 1992; Kim & Rees, 1992a) and the MoFeP from *Clostridium pasteurianum* (Bolin et al., 1993; Kim et al., 1993) have provided high-resolution structures for both proteins, along with their respective metal clusters. A structure for the FeP-MoFeP complex has not been achieved, so little is known about how these 2 proteins interact. Models for how these 2 proteins might dock for electron transfer have been suggested from analysis of the individual structures and from the position of the respective metal centers (Kim et al., 1992; Howard, 1993; Rees et al., 1993; Kim & Rees, 1994). In addition, chemical crosslinking studies (Willing et al., 1989; Willing & Howard, 1990) and site-directed mutagenesis studies of amino acids on both the FeP and the MoFeP have implicated Arg 100 (Chang et al., 1988; Lowery et al., 1989; Wolle et al., 1992b) and Glu 112 (Willing & Howard, 1990) of the FeP and MoFeP α-subunit Asp 161 (Kim et al., 1992) and β-subunit Phe 125 (Fisher et al., 1992) in docking. In the present work, data are presented revealing that the 2 positively charged amino acids, Arg 140 and Lys 143, of *A. vinelandii* nitrogenase FeP function in FeP-MoFeP docking. This has been accomplished by changing each amino acid by site-directed mutagenesis to the neutral amino acid glutamine and characterizing the properties of the purified, altered proteins. A significant role for each of these amino acids in component docking is demonstrated. It is additionally suggested that these residues play a role in the final alignment of the FeP and MoFeP complex before intercomponent electron transfer can occur (see Kinemage 1).

Results

Site-directed mutagenesis of the A. vinelandii nitrogenase FeP

An analysis of the FeP crystal structure (Georgiadis et al., 1992) reveals at least 3 stretches of amino acids that might be involved in MoFeP docking, namely residues 62–72, 97–120, and 138–144. Amino acids in each of these regions are located on the same surface of the FeP as the [4Fe-4S] cluster. Arg 100 and Glu 112, in the second region, have previously been implicated in docking (Chang et al., 1988; Lowery et al., 1989; Willing & Howard, 1990; Wolle et al., 1992b). In addition, Arg 100 is the site of ADP-ribosylation, a posttranslation modification mechanism used to regulate nitrogenase activity (Ludden & Roberts, 1989). Residues in the 138–144 region (P^{138}-I^{139}-R^{140}-E^{141}-N^{142}-K^{143}-A^{144}) form a loop structure that protrudes from the surface of the FeP near its [4Fe-4S] cluster (Fig. 1). Noteworthy among these residues are Arg 140, Glu 141, and Lys 143, all of which extend from the surface of the protein and all of which would be expected to be charged at physiological pH. Salt inhibition of FeP and MoFeP docking has suggested that ionic interactions are, in part, responsible for the docking process (Deits & Howard, 1990). In an attempt to probe the possible function of these 3 residues, each was changed to the neutral amino acid Gln by site-directed mutagenesis. Gln substitution would remove the charged residue and at the same time is predicted to be a conservative structural change (Bordo & Argos, 1991). Each of the altered FePs (R140Q, E141Q, K143Q) were expressed in *A. vinelandii* cells in place of the wild-type FeP. This was accomplished by replacing the chromosomal wild-type FeP gene, *nif H*, with the mutated gene by homologous gene recombination (Jacobson et al., 1989; Seefeldt & Mortenson, 1993). Cells expressing the E141Q FeP and wild-type MoFeP were found to grow at the same rate under nitrogen fixing conditions as cells expressing wild-type FeP, revealing that the charged residue Glu 141 was not essential to the function of the FeP. In contrast, cells expressing the R140Q or K143Q FeP, were found to grow very slowly under nitrogen-fixing conditions, suggesting that changing these residues had a significant effect on the function of the FeP.

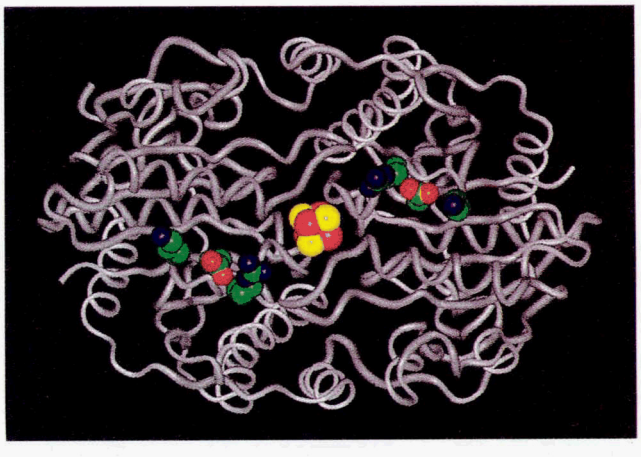

Fig. 1. Top view of nitrogenase FeP highlighting the positions of Arg 140, Glu 141, and Lys 143 and the [4Fe-4S] cluster. The view is down the 2-fold axis of symmetry from the [4Fe-4S] side. The α-carbon backbone is shown as a gray ribbon. The [4Fe-4S] cluster is shown with the inorganic sulfur in yellow and the iron in pink. The side chains for Arg 140, Glu 141, and Lys 143 are shown in color. The carbon atoms are in green, oxygen in red, and nitrogen in dark blue. Arg 140 is located closest to the central [4Fe-4S] cluster, Glu 141 next, and then Lys 143. The coordinates for the FeP were kindly provided by Dr. D.C. Rees of Caltech. Modeling was done on a Silicon Graphics Indigo System with the software INSIGHT.

To further probe the possible function of the Arg 140 and Lys 143 residues in FeP function, each of the altered proteins was purified to homogeneity and further characterized.

Activities of the R140Q and K143Q FePs

The substrate reduction activity of the wild-type FeP-MoFeP complex was compared to that of the R140Q FeP-MoFeP and K143Q FeP-MoFeP complexes. The altered proteins were found to support substantially decreased acetylene reduction rates when combined with wild-type MoFeP. Figure 2 shows the effects of varying the FeP concentration on the total rate of substrate reduction at a fixed MoFeP concentration. As can be seen, the R140Q FeP supported a maximal rate of 38% of the wild-type rate and the K143Q FeP supported a maximal rate 25% of wild type. Clearly, changing Arg 140 and Lys 143 to the neutral Gln has had a significant effect on the ability of the FeP to support substrate reduction when bound to the MoFeP.

Affinity of R140Q and K143Q FeP for the MoFeP

The results presented in Figure 2 reveal a possible reason for the lower activity of the altered FePs. In this experiment, a fixed quantity of MoFeP was titrated with increasing quantities of FeP. From the saturation curve, the kinetic affinity (K_{FeP}) of the FeP for the MoFeP can be defined as the concentration of FeP that gives half-maximal activity. It is clear from Figure 2 that both the R140Q and K143Q FeP have a significantly reduced kinetic affinity for binding to the MoFeP. Table 1 summarizes the experimentally determined K_{FeP} values derived from the data in Figure 2. Substituting Gln for Arg 140 has reduced the affinity of the FeP for the MoFeP by a factor of 11 when compared to the wild-type complex, and changing Lys 143 to Gln has reduced the affinity for binding to the MoFeP by a factor of 19. These results suggest that one consequence of changing both Arg 140 and Lys 143 to the neutral amino acid Gln is to reduce the affinity for docking to the MoFeP.

This possibility was further explored by analysis of the effects of salt concentration on FeP-MoFeP complex formation. It has been previously shown that increased ionic strength reduces the affinity of FeP binding to the MoFeP (Deits & Howard, 1990). This has been interpreted to suggest that ionic interactions are essential to the docking of the 2 proteins. Figure 3 shows the effect of increasing concentrations of NaCl on the substrate reduction rates of the wild-type FeP, and substituted FeP when complexed with wild-type MoFeP. The wild-type complex shows an initial increase in activity upon increasing NaCl concentrations, followed by a steady decrease in activity to 450 mM NaCl. The K143Q FeP-MoFeP complex showed a similar change in activity, however, the complex was significantly more sensitive to NaCl inhibition. The R140Q FeP-MoFeP complex showed a dramatic decrease in activity at low NaCl concentrations. These effects were quantified by determining the concentration of NaCl required to cause 50% inhibition of the noninhibited rate. The apparent inhibition constants ($K_{I(NaCl)}$) are summarized in Table 1. The K143Q FeP-MoFeP complex was 2.2 times more sensitive to NaCl inhibition than the wild-type complex and the R140Q FeP-MoFeP complex was 7.2 times more sensitive to NaCl inhibition. This increased sensitivity to NaCl is comparable to that found for FeP in which Arg 100 was changed to His (Wolle et al., 1992b). These results suggest that Arg 140 and Lys 143 participate in ionic interactions essential to docking with the MoFeP, and that changing each to the neutral Gln makes the complex more sensitive to NaCl inhibition. This is consistent with the conclusion from the FeP titration experiment.

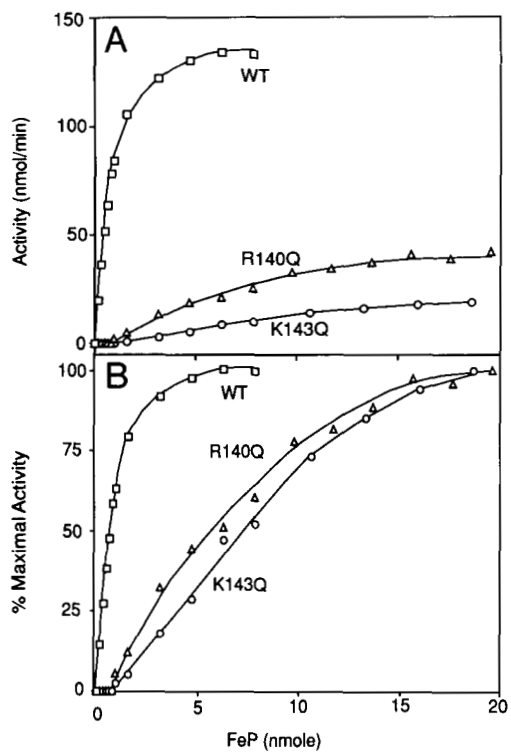

Fig. 2. Dependence of nitrogenase acetylene reduction activity on the concentration of FeP. Acetylene reduction activity was determined under low salt conditions as described in Materials and methods. Each assay contained 64 μg (0.256 nmol) of wild-type MoFeP and the indicated quantities of either wild-type FeP (□), R140Q FeP (△), or K143Q FeP (○). **A:** Acetylene reduction activity measured as nanomoles ethylene formed per minute was plotted as a function of the quantity of FeP. **B:** The percentage of the maximal activity for each FeP-MoFeP complex was plotted against the quantity of FeP added.

Table 1. *Summary of kinetic constants for iron proteins*

Iron protein	V_{max}[a] (nmol ethylene·min^{-1})	K_{FeP}[b] (μM)	Fold increase in K_{FeP}	K_{MgATP}[c] (μM)	$K_{I(NaCl)}$[d] (mM)
WT	200	1.4	–	240	230
R140Q	77	14.8	11	825	32
K143Q	50	27.0	19	1,000	105

[a] Maximum rate calculated for saturating FeP and 64 μg (0.256 nmol) of MoFeP.

[b] Calculated concentration of FeP that gives half-maximal activity with 64 μg (0.256 nmol) of MoFeP.

[c] Concentration of MgATP that gives half-maximal activity with 130 μg (0.520 nmol) of MoFeP and 450 μg (7.03 nmol) of FeP.

[d] Concentration of NaCl required to give half the activity of the no NaCl added sample. Assays contained 64 μg (0.256 nmol) of MoFeP and 250 μg (3.91 nmol) of FeP.

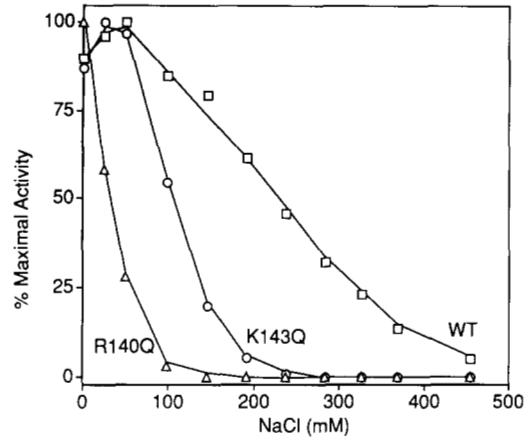

Fig. 3. The inhibition of nitrogenase-catalyzed acetylene reduction by NaCl. Acetylene reduction activity was determined as described in the Materials and methods. Each assay contained 64 μg (0.256 nmol) of wild-type MoFeP and 250 μg (3.91 nmol) of either wild-type FeP (□) or R140Q FeP (△) or K143Q FeP (○) in 1 mL liquid volume. NaCl was added to the final concentration indicated from a 5 M stock solution. The percentage of the maximal activity was plotted against the concentration of NaCl.

Affinity of the R140Q and K143Q FeP-MoFeP complexes for MgATP

The affinity for MgATP in substrate reduction was investigated for each altered FeP-MoFeP complex. Figure 4 shows the effects of increasing MgATP concentration on the rates of substrate reduction for each nitrogenase complex. As can be seen, the wild-type complex saturated for MgATP with a MgATP concentration required to support half-maximal activity (K_{MgATP}) calculated to be 240 μM (Table 1). Both the K143Q FeP- and R140Q FeP-MoFeP complexes saturated for MgATP in substrate reduction reactions at higher MgATP concentrations, with K_{MgATP} values 3.4- and 4.2-fold higher than the wild-type complex. This lower kinetic affinity of the altered FePs for MgATP utilization indicates that changing Arg 140 and Lys 143 to Gln has affected the efficiency of MgATP utilization by the complex. These decreases in the kinetic affinity for MgATP utilization further suggest that Arg 140 and Lys 143 function in the formation of the FeP-MoFeP complex.

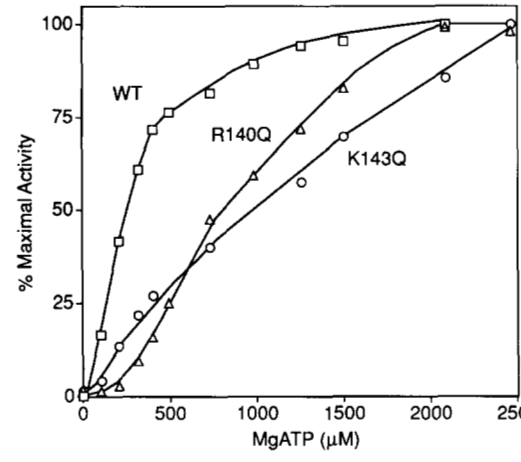

Fig. 4. Dependence of nitrogenase acetylene reduction activity on MgATP concentration. Acetylene reduction activity was determined as described in the Materials and methods. Each assay contained 130 μg (0.52 nmol) of wild-type MoFeP and 450 μg (7.0 nmol) of either wild-type (□) or R140Q (△) or K143Q (○) FeP in a liquid volume of 1 mL. MgATP was added to the final concentration indicated. The percentage of the maximal activity was plotted against the concentration of MgATP.

Fe^{2+} chelation from FeP by α,α'-dipyridyl and MoFeP protection

When wild-type FeP binds 2 MgATP, the protein is known to undergo conformational changes that result in changes in the environment of the [4Fe-4S] cluster (Mortenson et al., 1993). These changes in the [4Fe-4S] cluster have been suggested to be a prerequisite to the intercomponent electron transfer reaction. One indicator of this change in the [4Fe-4S] cluster of the FeP is its increased susceptibility to chelation by iron-specific chelators when MgATP binds to the FeP (Walker & Mortenson, 1974). If the FeP is incubated in the presence of the iron chelator α,α'-dipyridyl, no chelation of Fe^{2+} from the cluster is observed. When MgATP is added, however, a time-dependent chelation of the iron occurs that can be followed in real-time as an increased absorbance at 520 nm resulting from the formation of the colored complex Fe^{2+}-α,α'-dipyridyl (Walker & Mortenson, 1974). A conformational change in the [4Fe-4S] cluster environment has been suggested to result in an increased accessibility to the chelator. This increased accessibility, until now, has been a good indicator for the potential for intercomponent electron transfer. We have investigated this MgATP-dependent chelation reaction for both the R140Q and the K143Q FePs as one way to further probe the functional consequences of changing these amino acids. Figure 5A shows the time-dependent chelation of Fe^{2+} by α,α'-dipyridyl from wild-type and the altered FePs, both before and after MgATP addition. As expected, the wild-type protein showed no Fe^{2+} chelation before MgATP was added. Following MgATP addition, a time-dependent chelation reaction was observed. Qualitatively, the R140Q FeP reacted similarly, except that the rate of Fe^{2+} chelation was faster than for the wild-type FeP. When the logarithm of the percentage of Fe^{2+} remaining bound to the wild-type FeP was plotted against the time after MgATP addition, a linear rate was observed, indicating an apparent first-order process. A similar apparent first-order rate of chelation was observed for the R140Q FeP, except that the apparent rate constant was 2.6 times faster than for the wild-type FeP (0.026 s^{-1} compared to 0.01 s^{-1}). The K143Q FeP also showed an apparent first-order rate of chelation, but with a significantly faster apparent first-order rate constant of 0.071 s^{-1} (Fig. 6). Inspection of the rate of Fe^{+2} chelation from the K143Q FeP prior to the addition of MgATP in Figure 5A revealed that Fe^{2+} was chelated from the K143Q FeP at a slow, but measurable rate even in the absence of MgATP. If allowed to continue for several minutes, all of the iron was eventually released (Fig. 5B). When MgATP was added after a fraction of the Fe^{2+} had been released in the absence of MgATP, the same final absorbance value was reached, indicating that the slow loss of Fe^{2+} comes from the [4Fe-4S] cluster and not advantageously bound Fe^{2+}.

Both the R140Q and K143Q FeP released the same total quantity of Fe^{2+} as the wild-type FeP (3.6 g-atoms of Fe per mol of

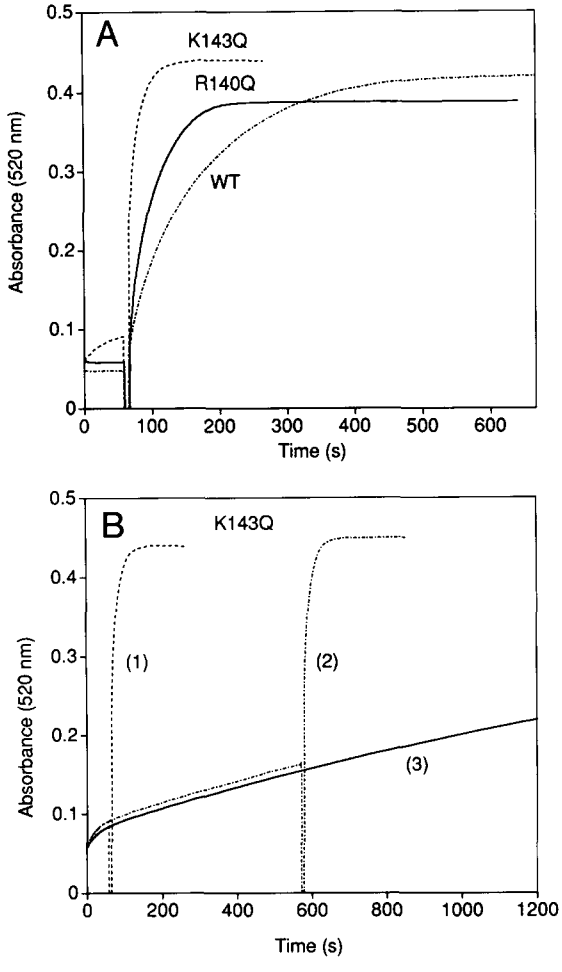

Fig. 5. Time course for the MgATP-dependent chelation of Fe^{2+} from iron proteins by α,α'-dipyridyl. Reaction conditions were as described in the Materials and methods. The absorbance at 520 nm of the Fe^{2+}-α,α'-dipyridyl complex versus time was recorded. **A:** Each reaction was initiated by addition of 0.9 mg of either wild-type (WT), R140Q, or K143Q FeP. At 60 s (downward spike), MgATP was added to a final concentration of 3.9 mM. **B:** Each reaction was initiated by the addition of 0.9 mg of K143Q FeP. MgATP was added to a final concentration of 3.9 mM at either 60 s (trace 1) or at 590 s (trace 2) or not at all (trace 3).

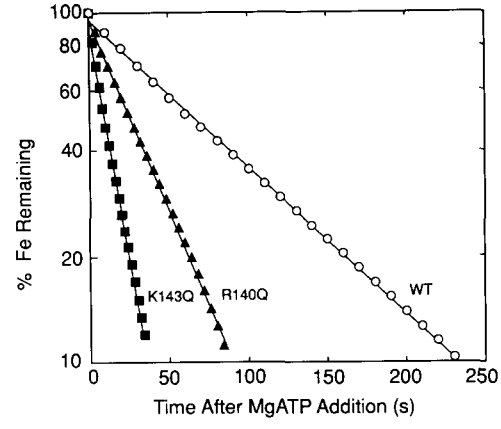

Fig. 6. The rate of MgATP-dependent Fe^{2+} chelation from iron proteins by α,α'-dipyridyl. The logarithm of the percentage of total releasable iron remaining bound to the FeP versus time after MgATP addition was plotted for each data set in Figure 5A. The apparent first-order rate constants were determined (K_{ob}): Wild-type FeP (WT, ○), K_{ob} = 0.01 s^{-1}; R140Q FeP (▲), K_{ob} = 0.026 s^{-1}; K143Q FeP (■), K_{ob} = 0.071 s^{-1}.

FeP), indicating that Fe was not lost during purification and that each protein contained a full complement of [4Fe-4S] cluster. This was confirmed by the presence of normal EPR spectra for both altered proteins (data not shown).

Earlier it had been shown that inclusion of MoFeP with the FeP in the chelation reaction resulted in a slower rate of Fe^{2+} chelation (Walker & Mortenson, 1974). This has been attributed to MoFeP binding to the FeP and thus protecting the [4Fe-4S] cluster from chelation by the chelator (Walker & Mortenson, 1974). During catalysis, the FeP would be bound a portion of the time to the MoFeP, which would protect the [4Fe-4S] cluster of the FeP from chelation. After the FeP releases from the MoFeP, it would be free in solution and thus susceptible to chelation. The result should be a decreased, but not zero, rate of Fe^{2+} chelation from FeP when MoFeP is present. Figure 7A shows the results of an experiment in which the wild-type FeP and MoFeP were mixed in a 2-to-1 ratio in an α,α'-dipyridyl chelation reaction. The presence of the MoFeP was found to result in a considerable decrease in the rate of chelation of Fe^{2+} from the FeP. An ATP-regenerating system was included in the reaction to prevent the formation of MgADP, which would compete for MgATP binding to the FeP. The MoFeP alone showed no Fe^{2+} chelation. This MoFeP protection was quantified by comparing apparent first-order rate constants for Fe^{2+} chelation in the presence or absence of MoFeP (Fig. 8). Similar experiments were also performed for the K143Q and R140Q FeP in the absence or presence of stoichiometric quantities of wild-type MoFeP (Fig. 7B,C). It can be seen from these data that the addition of MoFeP to the reaction mixture of the altered FePs had little or no effect on the rate or extent of Fe^{2+} release from the altered FePs. The apparent first-order rate constants for Fe^{2+} chelation were unchanged when MoFeP was present or absent (Fig. 8). These data clearly indicate that changing the positively charged Arg 140 and Lys 143 of the *A. vinelandii* FeP has resulted in a reduced affinity of the FeP for the MoFeP.

Coupling MgATP hydrolysis to electron transfer for the R140Q and K143Q FeP-MoFeP complexes

Under optimal conditions, the wild-type FeP-MoFeP complex hydrolyzes 2 MgATP for each electron transferred between the component proteins (Jeng et al., 1970). As a way to determine the coupling of these 2 processes for the altered proteins, electron transfer rates and MgATP hydrolysis rates were determined for the wild-type nitrogenase complex and for the R140Q and K143Q FeP-MoFeP complexes. The results are summarized in Table 2. As can be seen, the total electron transfer rates from R140Q and K143Q FeP to MoFeP were significantly lower than between the wild-type proteins. The total rates of MgATP hydrolysis were also reduced, but to a lesser extent than the electron transfer rates. The net result was a significantly higher ratio of MgATP hydrolyzed per electron transferred for the altered FePs. The wild-type FeP-MoFeP complex hydrolyzed 2.5

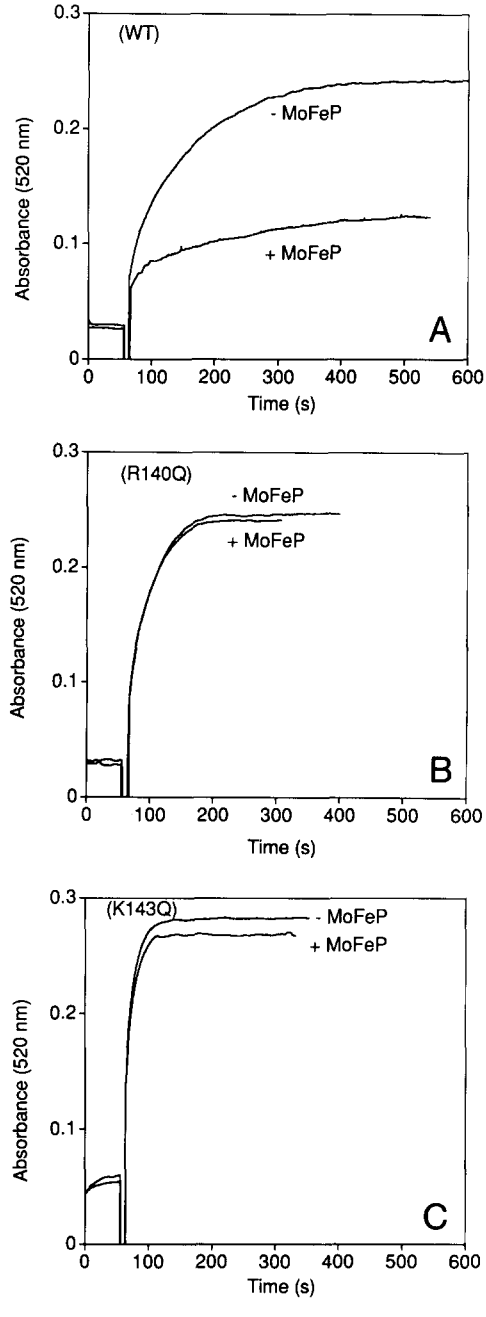

Fig. 7. MoFeP protection of MgATP-dependent Fe^{2+} chelation from FePs: Reaction conditions were as described in the Materials and methods. The reaction solution included phosphocreatine and creatine phosphokinase. Prior to the addition of FeP, wild-type MoFeP (0.92 mg or 3.6 nmol) was either added (+MoFeP) or not added (−MoFeP). The reaction was initiated by the addition of 470 μg (7.3 nmol) of the indicated FeP. At 60 s (downward spike), MgATP was added to a final concentration of 3.9 mM. **A:** Wild-type FeP. **B:** R140Q FeP. **C:** K143Q FeP.

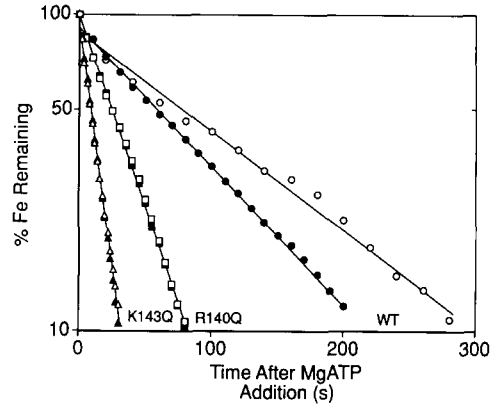

Fig. 8. The rate of Fe^{+2} chelation by α,α'-dipyridyl from FePs in the presence or absence of MoFeP. The logarithm of the percentage of total releasable iron remaining bound to the FeP versus time after MgATP addition was plotted for each data set in Figure 7A, B, and C. Closed symbols represent reactions in the absence of MoFeP, whereas open symbols represent reactions in the presence of MoFeP. Wild-type FeP (WT, circles), R140Q FeP (squares), and K143Q FeP (triangles). Apparent first-order rate constants (K_{ob}) were: Wild-type in the presence of MoFeP (○), 0.0086 s^{-1}; wild-type in the absence of MoFeP (●), 0.01 s^{-1}; R140Q FeP in the presence (□) or absence of MoFeP (■), 0.028 s^{-1}; K143Q FeP in the presence (△) or absence of MoFeP (▲), 0.089 s^{-1}.

MgATP for each electron transferred. In contrast, the R140Q and K143Q FeP-MoFeP complexes hydrolyzed 6.0 and 31 MgATP per electron transferred, respectively. These results are consistent with Arg 140 and Lys 143 functioning in the FeP-MoFeP interaction, particularly in the interaction required for electron transfer.

Discussion

The results presented in this work reveal that the positively charged amino acids Arg 140 and Lys 143 of the *A. vinelandii* FeP play a key role in docking to the MoFeP, a prerequisite to MgATP hydrolysis, intercomponent electron transfer, and substrate reduction.

These results can be integrated into a consensus model for how the FeP and MoFeP might interact. The current model holds that the FeP transfers an electron to the 8Fe cluster of the MoFeP, which in turn transfers 1 or 2 electrons to the FeMoco for substrate reduction (Thorneley & Lowe, 1985; Lowe et al., 1993). Thus, a model for FeP and MoFeP binding would require that the [4Fe-4S] cluster of the FeP bind near the 8Fe cluster of the MoFeP (Howard, 1993; Kim & Rees, 1994). A possible model for the docking of the FeP and MoFeP is illustrated in Kinemage 1. The recent X-ray crystal structure of the MoFeP from *A. vinelandii* allows analysis of the protein environment around the 8Fe cluster of MoFeP (Rees et al., 1993). The 8Fe cluster is bound between the MoFeP α- and β-subunits approximately 10 Å below the surface (Kim & Rees, 1994). Amino acids located at the surface near the 8Fe cluster include a series of hydrophobic residues (α Phe 125, β Phe 125, α Phe 186, β Phe 189, α Leu 158, β Val 157, β Ile 158, and β Ile 123) and a series of acidic residues (α Asp 162, β Asp 161, α Asp 128, α Asp 161, and β Glu 156) (Kim & Rees, 1992a). There is an approximate 2-fold axis of symmetry through the 8Fe cluster, with these amino acid residues arranged symmetrically around the cluster. Recent site-directed mutagenesis studies on β Phe 125 (Fisher et al., 1992) and α Asp 162 (Kim et al., 1992) near the 8Fe cluster of the MoFeP protein suggest that these residues function in binding to the FeP. The negatively charged residues near the MoFeP 8Fe cluster are tempting candidates for interaction with Arg 140 and Lys 143 of the FeP. Because the FeP is a homodi-

Table 2. *Coupling of MgATP hydrolysis to electron transfer by nitrogenase complexes*

FeP	Electron transfer rates[a] (nmol e^-/min/mg FeP)	MgATP hydrolysis rates[b] (nmol MgATP/min/mg FeP)	MgATP/e^-
WT	1,892 ± 82.7	4,841 ± 8,360	2.5
R140Q	151 ± 88.0	912 ± 862	6.0
K143Q	42 ± 82.8	1,316 ± 827	31

[a] Determined from the rate of the 2 electron reduction of C_2H_2 to C_2H_4. Each assay contained 0.93 nmol of wild-type MoFeP and 0.5 nmol of the noted FeP.
[b] Determined as the rate of MgADP formation (see Materials and methods).

mer, with a 2-fold axis of symmetry through the [4Fe-4S] cluster (Georgiadis et al., 1992), each subunit contains an Arg 140 and Lys 143. These residues could interact with the acidic residues surrounding the 8Fe cluster of the MoFeP. In addition, 2 Arg 100 residues are located around the [4Fe-4S] cluster of the FeP. Thus, Arg 100, Arg 140, and Lys 143 form a ring of 6 positively charged residues surrounding the [4Fe-4S] cluster of the FeP. Previous work on Arg 100 of the FeP has demonstrated a role for this residue in docking to the MoFeP (Chang et al., 1988; Lowery et al., 1989; Wolle et al., 1992b). In addition, Arg 100 of the FeP is the site of ADP-ribosylation in nitrogenase from several photosynthetic nitrogen-fixing bacteria, where a modification of Arg 100 functions to switch off the enzyme under conditions where it is not needed (Ludden & Roberts, 1989). The addition of this ADP-ribose group probably acts to prevent Arg 100 interaction with its counterpart on the MoFeP, rendering the complex inactive. With this docking model, the distance between the 8Fe cluster of the MoFeP and the [4Fe-4S] cluster of the FeP is estimated to be 15 Å (Howard, 1993; Kim & Rees, 1994).

A major question that remains is "what happens within each protein during docking that activates the complex for MgATP hydrolysis and electron transfer?" Because the crystal structures of each nitrogenase component are uncomplexed structures, they provide limited insights into the mechanisms for these activations. Possible models are suggested, however, from combining knowledge of the structures with previous mutagenesis and kinetic studies and the results presented here. One important observation is that MgATP hydrolysis can be uncoupled from intercomponent electron transfer. Earlier work with heterologous FeP-MoFeP complexes showed that such complexes would hydrolyze MgATP, but would not transfer electrons (Smith et al., 1976; Emerich & Burris, 1978). Likewise, changing Arg 100 of the FeP was found to uncouple MgATP hydrolysis from intercomponent electron transfer (Lowery et al., 1989; Wolle et al., 1992b). The data presented in this work show that Arg 140 and Lys 143 of the FeP and their interaction with the MoFeP are critical for coupling MgATP hydrolysis to electron transfer. Changing Arg 140 and Lys 143 resulted in a significant uncoupling of these 2 processes, with the altered proteins catalyzing the hydrolysis of up to 31 MgATP for each electron transferred. These data suggest a model in which MoFeP and FeP docking occurs in sequential steps. It would seem that at least 3 such states are required. These might include an initial docking complex, which further aligns to create a state competent for MgATP hydrolysis, which would be followed by a state competent for electron transfer. Similar models have been proposed for FeP and MoFeP interactions (Lowery et al., 1989; Howard, 1993).

In the formation of the initial complex, the 2 proteins would form a complex that is not ideally aligned for catalysis. The interaction of Glu 112 of the FeP and β-Lys 399 of the MoFeP might be involved in this initial recognition (Howard, 1993). Previous crosslinking studies between the FeP and the MoFeP protein have shown that Glu 112 of the FeP crosslinks to β-Lys 399 (Willing & Howard, 1990). Glu 112 is located in a patch of acidic amino acids on the FeP surface near the [4Fe-4S] cluster and β-Lys 399 is located on the MoFeP near the 8Fe cluster (Georgiadis et al., 1992). This crosslinking was found to be independent of the presence of MgATP (Willing et al., 1989) and did not require active FeP (Seefeldt et al., 1992), suggesting that it was part of an initial recognition complex.

Following the initial binding, the 2 proteins would further align by the interaction of additional amino acids on each protein (see Kinemage 1). This interaction would activate the FeP for MgATP hydrolysis. This state would be analogous to the heterologous *Clostridium pasteurianum* FeP-*A. vinelandii* MoFeP complex that catalyzes MgATP hydrolysis, but not electron transfer (Smith et al., 1976; Emerich & Burris, 1978). Although the FeP can bind 2 MgATP molecules, only the complex of the FeP and the MoFeP will hydrolyze MgATP. This suggests that docking of the component proteins results either in changes in the FeP that allow MgATP hydrolysis or completion of the catalytic site by the MoFeP. Binding of MgATP to the FeP would be a prerequisite for this second binding state. It is known that MgATP binding to the FeP induces conformational changes within the protein that result in changes in the properties of its [4Fe-4S] cluster. These conformational changes have been monitored by changes in EPR line shape of the [4Fe-4S] cluster (Orme-Johnson et al., 1972; Zumft et al., 1972), a change in the midpoint potential of the cluster by −150 mV (Watt et al., 1986), changes in the CD spectrum (Stephens et al., 1979), shifts in the NMR resonances of protons magnetically coupled to the paramagnetic [4Fe-4S] cluster (Meyer et al., 1988), changes in scattering of X-rays (Chen et al., 1994), and in Fe^{2+} chelation (Walker & Mortenson, 1974). This conformation of the FeP would be required for the formation of the second, MgATP hydrolytic state, with the MoFeP. It is interesting to note that the conformational changes that occur in the FeP when MgATP binds, which result in increased accessibility of the [4Fe-4S] cluster to chelation by α,α′-dipyridyl, does not seem to be a good predictor of the rate of intercomponent electron transfer. The R140Q and K143Q FeP investigated in this study showed sig-

nificantly faster Fe^{2+} chelation rates than wild-type FeP, yet showed much slower electron transfer rates.

Based on the X-ray structure and site-directed mutagenesis studies of the FeP, it is known that MgATP binds to a nucleotide binding amino acid motif in the FeP that includes Lys 15 (Seefeldt et al., 1992), Ser 16 (Seefeldt & Mortenson, 1993), and Asp 125 (Wolle et al., 1992a). This phosphate binding pocket is located approximately 19 Å from the FeP cluster and the face of the FeP that would include Arg 140, Lys 143, and Arg 100 (Georgiadis et al., 1992). How, then, does binding of the MoFeP 19 Å from the phosphate binding site activate the hydrolytic mechanism? It seems likely that MoFeP docking results in conformational changes within the FeP that could be transmitted to the phosphate binding site, possibly moving amino acids (e.g., Asp 39 and Asp 43) into position to catalyze the hydrolysis of MgATP.

After formation of the complex state for MgATP hydrolysis, further alignment would create the complex state for electron transfer. Arg 100, Arg 140, and Lys 143 of the FeP, through their interactions with residues on the MoFeP, seem to play a significant role in this alignment of the 2 proteins. A similar, multistep model for binding of other electron transfer proteins has been suggested (Qin & Kostic, 1993; Gray & Ellis, 1994). It is reasonable to assume that conformational changes are induced within both component proteins at this stage in docking, which could induce changes near or between the clusters that would facilitate electron transfer. Such changes might include movement of amino acids to create pathways for electron transfer or to change the properties (e.g., midpoint potentials) of each cluster. The faster rates of Fe^{2+} chelation from the K143Q and R140Q FeP when MgATP is bound suggest that these residues might move closer to the [4Fe-4S] cluster in the MgATP-bound state. In this case, changing these charged residues to the neutral Gln might be imagined to allow the chelator greater access to the cluster by eliminating charge repulsion of the chelator.

Although the FeP-MoFeP complex can hydrolyze MgATP without electron transfer, the reverse is not true. The exact function of MgATP hydrolysis in activating electron transfer is unknown, but, again, probably involves conformational changes within each protein (Howard, 1993). Two possible models have been suggested in which these conformational changes facilitate electron transfer either from the FeP to the 8Fe cluster followed by electron transfer to FeMoco or in which the electron is transferred from the 8Fe cluster to FeMoco followed by transfer from the FeP to the 8Fe cluster (Kim & Rees, 1994).

The studies presented in this work demonstrate that the basic amino acids Arg 140 and Lys 143 of the FeP function in docking with the MoFeP, possibly through interactions with acidic amino acids near the 8Fe cluster of the MoFeP (see Kinemage 1). A detailed description of the events involved in this complex process will be the focus of future work.

Materials and methods

Site-directed mutagenesis, expression, and purification of altered FePs

Oligonucleotide-directed mutagenesis of the *A. vinelandii* nitrogenase FeP gene, *nifH*, was carried out as previously described (Seefeldt et al., 1992; Seefeldt & Mortenson, 1993). The mutated *nifH* gene was incorporated into the *A. vinelandii* chromosome in place of the wild-type *nifH* gene for overexpression (Jacobson et al., 1989; Seefeldt & Mortenson, 1993). Each altered FeP was expressed in *A. vinelandii* cells and purified to homogeneity as described (Seefeldt & Mortenson, 1993). Protein concentrations were determined by the modified biuret method using bovine serum albumin as standard (Chromy et al., 1974). All proteins used were homogeneous as judged by analysis on SDS gels stained with Coomassie blue (Seefeldt et al., 1992). The wild-type FeP and MoFeP proteins used had specific activities of 2,000 nmol acetylene reduced $\cdot \min^{-1} \cdot mg^{-1}$.

Activity assays

Nitrogenase-catalyzed acetylene reduction was used to determine substrate reduction rates for nitrogenase FeP and MoFeP complexes with the low salt assay described (Deits & Howard, 1990; Seefeldt & Mortenson, 1993) except that acetylene and ethylene were separated and quantified by gas chromatography on a Shimadzu GC-8A with a flame ionization detector fitted with a 1-ft × 1/8-in PoraPak N column with nitrogen as the carrier gas. The low salt assay mixture consisted of 25 mM Tris buffer, pH 8.0, with 2 mM ATP, 2.5 mM $MgCl_2$, 6 mM creatine phosphate, 0.125 mg $\cdot$ mL^{-1} creatine phosphokinase, 10 mM dithionite ($S_2O_4^{2-}$), and 1.25 mg $\cdot$ mL^{-1} bovine serum albumin. For the FeP titration experiments, a fixed quantity of wild-type MoFeP was added to each assay vial and the reaction was initiated by addition of a defined quantity of FeP (Seefeldt & Mortenson, 1993). For MgATP titration experiments, ATP was omitted from the assay mixture and a defined amount of ATP was added to each assay vial (Seefeldt & Mortenson, 1993). FeP and MoFeP were added to initiate the reaction. For the NaCl titration experiment, defined quantities of NaCl from a 5 M stock solution were added to each assay vial (Deits & Howard, 1990).

MgATP hydrolysis and electron transfer rates

The coupling of MgATP hydrolysis to electron transfer was determined by quantifying the rates of acetylene reduction and MgADP formation in a single assay vial. To a 9.3-mL volume serum vial was added 1 mL of assay buffer (80 mM TES buffer, pH 7.0, with 1 mg/mL bovine serum albumin and 2 mM MgATP). The capped vial was evacuated and flushed with argon and acetylene was added to a final 8.4% of the gas volume. Dithionite ($Na_2S_2O_4$) was added to a final concentration of 10 mM and the reaction was initiated by the addition of the indicated quantity of MoFeP and FeP. The reaction was allowed to proceed at 30 °C with shaking and was terminated by addition of 250 μL of 2.5 M H_2SO_4. An aliquot of the gas phase was used to quantify acetylene and ethylene by gas chromatography as outlined above. Five-hundred microliters of the liquid from the assay vial was centrifuged at 14,000 × g for 3 min to remove precipitated materials. An aliquot of the supernatant was used for the HPLC separation and quantification of ADP and ATP as previously described (Seefeldt & Mortenson, 1993).

MgATP-dependent Fe-chelation from FeP

The MgATP-dependent chelation of Fe^{2+} from FeP was monitored spectrophotometrically as previously described by following the formation of the colored complex of Fe^{2+}-α,α'-dipyridyl

with an extinction coefficient of 8,400 $M^{-1} \cdot cm^{-1}$ at 520 nm (Walker & Mortenson, 1974; Seefeldt et al., 1992). All reactions were done in the absence of oxygen in a reaction volume of 1 mL total. The assay solution consisted of 35 mM Tris buffer, pH 8.0, with 6.25 mM α,α'-dipyridyl, and 1.3 mM dithionite. At the indicated time, MgATP was added to a final concentration of 3.9 mM. All spectrophotometric measurements were performed on a Hewlett-Packard 8452A diode array spectrophotometer interfaced to a computer for data acquisition.

To determine the effects of MoFeP on the rate of Fe^{2+} chelation from FeP, the assay solution was modified to include 6 mM creatine phosphate and 0.125 mg/mL of creatine phosphokinase to prevent the formation of MgADP. A defined quantity of MoFeP was added to the assay vial prior to the introduction of the FeP. MgATP was added at the indicated times.

Acknowledgments

This work was supported by National Science Foundation grant MCB-9315835. I thank Dr. Leonard E. Mortenson for helpful discussions, Sandra Gay for technical assistance, and Dr. Gerard Jensen for assistance with the computer graphic image in Figure 1. I also thank Beth Cader Villafranca for assistance with the kinemage.

References

Bolin JT, Ronco A, Morgan TV, Mortenson LE, Xuong NH. 1993. The unusual metal clusters of nitrogenase: Structural features revealed by X-ray anomalous diffraction studies of the MoFe protein from *Clostridium pasteurianum*. *Proc Natl Acad Sci USA 90*:1078–1082.

Bordo D, Argos P. 1991. Suggestions for "safe" residue substitutions in site-directed mutagenesis. *J Mol Biol 217*:721–729.

Burris RH. 1991. Nitrogenase. *J Biol Chem 266*:9339–9342.

Chang CL, Davis LC, Rider M, Takemoto DJ. 1988. Characterization of *nifH* mutations of *Klebsiella pneumoniae*. *J Bacteriol 170*:4015–4022.

Chen L, Gavini N, Tsuruta H, Eliezer D, Burgess BK, Doniach S, Hodgson KO. 1994. MgATP-induced conformational changes in the iron protein from *Azotobacter vinelandii*, as studied by small-angle X-ray scattering. *J Biol Chem 269*:3290–3294.

Chromy V, Fischer J, Kulhanek V. 1974. Re-evaluation of EDTA-chelated biuret reagent. *Clin Chem 20*:1362–1363.

Dean DR, Bolin JT, Zheng L. 1993. Nitrogenase metalloclusters: Structures, organization, and synthesis. *J Bacteriol 175*:6737–6744.

Deits TL, Howard JB. 1990. Effects of salts on *Azotobacter vinelandii* nitrogenase activities. *J Biol Chem 265*:3859–3867.

Emerich DW, Burris RH. 1978. Complementary functioning of the component proteins of nitrogenase from several bacteria. *J Bacteriol 134*: 936–943.

Fisher K, Thorneley RNF, Lowe DJ, Pau RN. 1992. The role of β-Phe 124 of *K. pneumoniae* MoFe-protein in MgATP-dependent electron transfer from the Fe-protein. In: Palacios R, Mora J, Newton WE, eds. *New horizons in nitrogen fixation*. Norwell, Massachusetts: Kluwer Academic Publishers. pp 135–135.

Georgiadis MM, Komiya H, Chakrabarti P, Woo D, Kornuc JJ, Rees DC. 1992. Crystallographic structure of the nitrogenase iron protein from *Azotobacter vinelandii*. *Science 257*:1653–1659.

Gray HB, Ellis WR. 1994. Electron transfer. In: Bertini I, Gray HB, Lippard SJ, Valentine JS, eds. *Bioinorganic chemistry*. Mill Valley, California: University Science Books. pp 315–363.

Hageman RV, Burris RH. 1978. Nitrogenase and nitrogenase reductase associate and dissociate with each catalytic cycle. *Proc Natl Acad Sci USA 75*:2699–2702.

Howard JB. 1993. Protein component complex formation and adenosine triphosphate hydrolysis in nitrogenase. In: Stiefel EI, Coucouvanis D, Newton WE, eds. *Molybdenum enzymes, cofactors, and model systems*. Washington D.C.: American Chemical Society. pp 271–289.

Jacobson MR, Cash VL, Weiss MC, Laird NF, Newton WE, Dean DR. 1989. Biochemical and genetic analysis of the *nifUSVWZM* cluster from *Azotobacter vinelandii*. *Mol Gen Genet 219*:49–57.

Jeng DY, Morris JA, Mortenson LE. 1970. The effect of reductant in inorganic phosphate release from adenosine 5′-triphosphate by purified nitrogenase of *Clostridium pasteurianum*. *J Biol Chem 245*:2809–2813.

Kim CH, Zheng L, Newton WE, Dean DR. 1992. Intermolecular electron transfer and substrate reduction properties of MoFe proteins altered by site-specific amino acid substitution. In: Palacios R, Mora J, Newton WE, eds. *New horizons in nitrogen fixation*. Norwell, Massachusetts: Kluwer Academic Publishers. pp 105–110.

Kim J, Rees DC. 1992a. Crystallographic structure and functional implications of the nitrogenase molybdenum iron protein from *Azotobacter vinelandii*. *Nature 360*:553–560.

Kim J, Rees DC. 1992b. Structural models for the metal centers in the nitrogenase molybdenum-iron protein. *Science 257*:1677–1682.

Kim J, Rees DC. 1994. Nitrogenase and biological nitrogen fixation. *Biochemistry 33*:389–397.

Kim J, Woo D, Rees DC. 1993. X-ray crystal structure of the nitrogenase molybdenum-iron protein from *Clostridium pasteurianum* at 3.0-Å resolution. *Biochemistry 32*:7104–7115.

Lowe DJ, Fisher K, Thorneley RNF. 1993. *Klebsiella pneumoniae* nitrogenase: Pre-steady state absorbance changes show that redox changes occur in the MoFe protein that depend on substrate and component protein ratio; a role for P-centres in reducing nitrogen. *Biochem J 292*:93–98.

Lowery RG, Chang CL, Davis LC, McKenna MC, Stephens PJ, Ludden PW. 1989. Substitution of histidine for arginine-101 of dinitrogenase reductase disrupts electron transfer to dinitrogenase. *Biochemistry 28*:1206–1212.

Ludden PW, Roberts GP. 1989. Regulation of nitrogenase activity by reversible ADP-ribosylation. *Curr Top Cell Regul 30*:23–55.

Meyer J, Gaillard J, Moulis JM. 1988. Hydrogen-1 nuclear magnetic resonance of the nitrogenase iron protein (Cp2) from *Clostridium pasteurianum*. *Biochemistry 27*:6150–6156.

Mortenson LE, Seefeldt LC, Morgan TV, Bolin J. 1993. The role of metal clusters and MgATP in nitrogenase catalysis. *Adv Enzymol 67*:299–373.

Orme-Johnson WH. 1992. Nitrogenase structure: Where to now? *Science 257*:1639–1640.

Orme-Johnson WH, Hamilton WD, Jones TL, Tso MYW, Burris RH, Shah VK, Brill WJ. 1972. Electron paramagnetic resonance of nitrogenase and nitrogenase components from *Clostridium pasteurianum* W5 and *Azotobacter vinelandii* OP. *Proc Natl Acad Sci USA 69*:3142–3145.

Qin L, Kostic NM. 1993. Importance of protein rearrangement in the electron-transfer reaction between the physiological partners cytochrome *f* and plastocyanin. *Biochemistry 32*:6073–6080.

Rees DC, Chan MK, Kim J. 1993. Structure and function of nitrogenase. *Adv Inorg Chem 40*:89–119.

Seefeldt LC, Morgan TV, Dean DR, Mortenson LE. 1992. Mapping the sites of MgATP and MgADP interactions with the nitrogenase of *Azotobacter vinelandii*: Lysine 15 of the iron protein plays a major role in MgATP interaction. *J Biol Chem 267*:6680–6688.

Seefeldt LC, Mortenson LE. 1993. Increasing nitrogenase catalytic efficiency for MgATP by changing serine 16 of its Fe protein to threonine: Use of Mn^{2+} to show interaction of serine 16 with Mg^{2+}. *Protein Sci 2*:93–102.

Smith BE, Eady RR. 1992. Metalloclusters of the nitrogenases. *Eur J Biochem 205*:1–15.

Smith BE, Thorneley RNF, Eady RR, Mortenson LE. 1976. Nitrogenase from *Klebsiella pneumoniae* and *Clostridium pasteurianum*. *Biochem J 157*: 439–447.

Stephens PJ, McKenna CE, Smith BE, Nguyen HT, McKenna MC, Thomson AJ, Devlin F, Jones JB. 1979. Circular dichroism and magnetic circular dichroism of nitrogenase proteins. *Proc Natl Acad Sci USA 76*: 2585–2589.

Thorneley RNF, Lowe DJ. 1985. Kinetics and mechanisms of the nitrogenase enzyme system. In: Spiro TG, ed. *Molybdenum enzymes*. New York: Wiley. pp 221–284.

Walker GA, Mortenson LE. 1974. Effect of magnesium adenosine 5′-triphosphate on the accessibility of the iron of clostridial azoferredoxin, a component of nitrogenase. *Biochemistry 13*:2382–2388.

Watt GD, Wang ZC, Knotts RR. 1986. Redox reactions of and nucleotide binding to the iron protein of *Azotobacter vinelandii*. *Biochemistry 25*: 8156–8162.

Willing AH, Georgiadis MM, Rees DC, Howard JB. 1989. Cross-linking of nitrogenase components. *J Biol Chem 264*:8499–8503.

Willing AH, Howard JB. 1990. Crosslinking site in *Azotobacter vinelandii* complex. *J Biol Chem 265*:6596–6599.

Wolle D, Dean DR, Howard JB. 1992a. Nucleotide iron–sulfur cluster signal transduction in the nitrogenase iron-protein—The role of Asp(125). *Science 258*:992–995.

Wolle D, Kim CH, Dean D, Howard JB. 1992b. Ionic interactions in the nitrogenase complex: Properties of Fe-protein containing substitutions for Arg-100. *J Biol Chem 267*:3667–3673.

Zumft WG, Cretney WC, Huang TC, Mortenson LE, Palmer G. 1972. On the structure and function of nitrogenase from *Clostridium pasteurianum* W5. *Biochem Biophys Res Commun 48*:1525–1532.